



OPEN

Research on methods for controlling strand sag in main cables

Pingming Huang, Chongjin Li[✉] & Hanzheng Xu

The accuracy of main cable construction in suspension bridges is directly influenced by the sag of the strands during the erection process. Thus, effective methods for controlling strand sag are crucial. However, the current control standards and methods are primarily based on practical engineering experience, lacking quantitative analysis and a sufficient basis. This paper aims to address this gap by summarizing four commonly used strand sag control methods and proposing a quantitative analysis model that considers the influence of random factors. The model quantifies the impact of these methods on the main cable shape and strand tension after cable tightening. To illustrate the practical application, a suspension bridge is utilized as a case study. The results of the study illustrate a linear relationship between the main cable sag and inter-strand distance, with each control method exhibiting a varying linear change rate. Moreover, the discrepancy in strand distance contributes to uneven strand tension after cable tightening. Random errors contribute to the dispersion of the main cable sag and strand tension, which are further exacerbated by cumulative errors between layers of general strands. Based on the study's results, this paper provides valuable references for the erection and control of the main cable in suspension bridges.

Keywords Sag control, Inter-strand distance, Cable tightening, Strand tension, Non-uniformity

Once the main cable is erected, its shape becomes difficult to change, and any errors in the initial cable shape will have a significant impact on the subsequent construction stages^{1,2}. The main cable erection methods for a suspension bridge are air spinning (AS) and the prefabricated parallel wire strand (PPWS) method³. In the AS method, steel wires are utilized as the traction unit, with multiple wires being assembled into a strand in the catwalk, followed by the bundling of multiple strands to form the main cable. In contrast, the PPWS method employs the cable strand as the traction unit, with strands being directly bound together to create the main cable. Compared with the AS method, PPWS has the advantage of fast construction speed⁴, and it is widely used in Japan and China⁵⁻⁷. Strand sag control in the construction process is the key to ensuring the quality of the main cable erection³. Currently, the increasing span of suspension bridges and the increasing diameter of main cables pose challenges to the quality of main cable installation⁸.

The current mature control method^{9,10} uses the first strand as the reference strand. Its shape is controlled based on the absolute elevation, while the general strands are controlled based on the relative elevation difference from the reference strand. For the erection of general strands, it is generally necessary to achieve the ideal state of “half approaching, half separation” between adjacent strands, where the inter-strand distance is zero. However, in the case of a suspension bridge built in Southwest China, the ideal state was not achieved when the strands were erected according to the principle of “half approaching, half separation”¹¹. Inaccurate measurements of the inter-strand distance and temperature will lead to unequal spacings between strand layers, resulting in the upper layer of strands pressing down the lower layer. The error accumulation will make the reference strand elongate due to increased force, so that the overall shape of the strands deviates from the theoretical value¹². Consequently, many projects have established requirements for the accuracy of cable strand erection, as shown in Table 1.

It can be seen from Table 1 that there is no unified control standard for the erection accuracy of many projects, most of which are formulated considering previous projects¹⁸. To reduce the mutual interference between the strands in the erection process and change the fuzzy requirements of “half approaching, half separation”, some scholars have proposed quantifying the inter-strand distance. For example, during the erection of the Minami Bisan-Seto Bridge's reference strand in Japan⁶, the height of the reference strand was raised compared with the theoretical position based on experience, but no specific basis or numerical value was given. In the erection of the strands of the Miaozui Yangtze River Bridge¹⁹, all the general strands were raised by 3 cm compared with the

School of Highway, Chang'an University, Xi'an 710064, China. ✉email: chjinli@126.com

Bridge	Allowable height difference between general strands and reference strand
Minami Bisan-Seto Bridge ⁶	-30 mm to 30 mm
Runyang Bridge ¹³ , Ma Anshan Bridge ¹⁴	0 to +5 mm
A self-anchored suspension bridge in China ¹⁵	0 to +15 mm
Aizhai Bridge ¹⁶	-5 mm to +5 mm
Wu Fengshan Yangtze River Bridge ¹⁷	-5 mm to +10 mm

Table 1. Control standards for the erection accuracy of various bridges.

reference strand to prevent the compression of the reference strand. The inter-strand distance of the Jin Dong Bridge²⁰ is the difference between the diameter of a circle with an area equal to that of the hexagon and the vertical separation between the top and bottom borders of the hexagon. During the erection of the strands of the Wu Fengshan Yangtze River Bridge¹⁷, the temperature differential of 0.5 °C determined how far apart the strands were in the main span's center, to ensure that the strands would not collide within a temperature range of 0.5 °C.

However, there is no quantitative analysis conclusion regarding the effectiveness of the aforementioned methods. Most of the current studies on the main cable shape are based on the main cable itself^{21–23}, and there is a lack of detailed analysis focusing on the individual strands. The inter-strand distance will directly lead to an increase in the distance between the uppermost and lowermost layers of the strands, which will further lead to a change in the main cable shape and the strand tension after cable tightening. The magnitude of these changes is of great concern. In response to the abovementioned issues, this paper summarizes the current four methods of strand sag control. It establishes a quantitative analysis model that considers random factors with the strand as the analysis object. Furthermore, a calculation program is developed. A suspension bridge was used as a case study to analyse the effects of the four methods on the main cable shape and the strand tension after cable tightening. Based on the analysis results, recommendations on control methods are provided to serve as a reference for the construction of the main cable. This paper quantifies the effect of different strand sag control methods on the main cable sag and strand tension after cable tightening. The selection of the method no longer simply relies on experience, and the inter-strand distance can be more scientifically formulated, which has practical significance for improving the accuracy of main cable erection.

Theoretical model of cable tightening

Basic equations

To simplify the calculation of the strand shape, it is assumed that there is a perfectly flexible cable between A and B, with uniform weight distribution along its length. The cable material complies with Hooke's law, and the changes in cross-section under load are neglected²⁴. The simplified mechanical model, considering only self-weight, is illustrated in Fig. 1. By applying mechanical equilibrium conditions and geometric relations²⁵, Eqs. (1) and (2) can be derived²⁶:

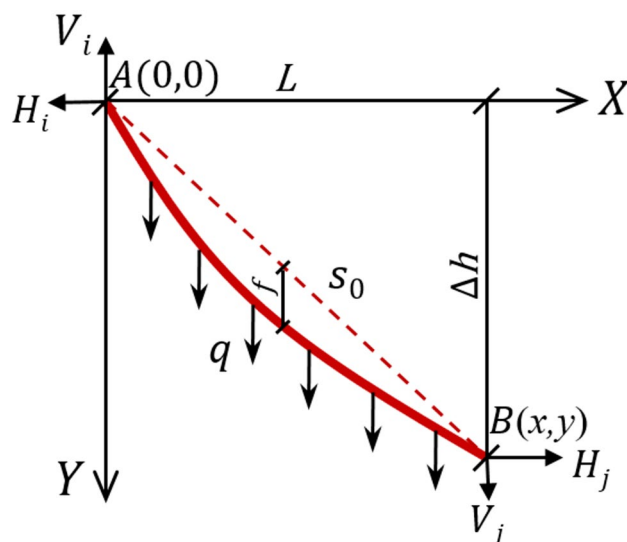


Figure 1. Simplified mechanical model of a cable under self-weight.

$$x(s_0) = -\frac{H_i \cdot s_0}{E \cdot A} - \frac{H_j}{q} \left[\ln \frac{q \cdot s_0 + V_i + \sqrt{(q \cdot s_0 + V_i)^2 + H_i^2}}{V_i + \sqrt{H_i^2 + V_i^2}} \right] \tag{1}$$

$$y(s_0) = -\frac{q \cdot s_0^2 + 2 \cdot V_i \cdot s_0}{2 \cdot E \cdot A} - \frac{1}{q} \left[\sqrt{(q \cdot s_0 + V_i)^2 + H_i^2} - \sqrt{H_i^2 + V_i^2} \right] \tag{2}$$

where: q represents the self-weight per unit length of the cable under the unstrained state. E , A , s_0 and f denote the elastic modulus, sectional area, unstrained length, and midpoint rise of the cable, respectively. $x(s_0)$ and $y(s_0)$ are the span (L) and height difference (Δh) of the cable segment. H_i and H_j represent the horizontal components at both ends of the cable tension, while V_i and V_j refer to the vertical components at both ends of the cable tension, respectively.

Equations (1) and (2), known as the basic equations of the cable state, describe the relationship between the internal force and the shape of the cable. The appropriate constraint conditions (3) should be selected for solving these equations based on the actual situation.

$$\begin{cases} x(s_0) = L \\ x(s_f) = L/2 \\ y(s_0) = \Delta h \\ y(s_f) = f + \Delta h/2 \end{cases} \tag{3}$$

where s_f represents the unstrained length between point A and the midpoint of the span ($L/2$).

Calculation principle and program implementation

The strands with different sags will be readjusted to have a unified sag after cable tightening, so the strands interact with each other due to mutual extrusion²⁷. The unstrained length of each strand before and after cable tightening is constant. Based on the principle of mass conservation, a portion of the self-weight load from a strand with a larger sag will be transferred to the strand with a smaller sag, ensuring consistency in the shape of each strand after cable tightening. According to the above principle, the theoretical calculation model of cable tightening is established without considering the influence of the lateral arrangement of the strands, which means that the difference in the strand spacing exists only in the vertical plane.

A main cable is composed of several strands. Let us consider the distance between points A and B as L , with a height difference of Δh . It is assumed that the strand spacing at the midpoint of the span differs from that at the saddle. The saddle position is equivalent to one point, and the corresponding sag of each strand is f_i . All strands will have the same sag (f_0) after cable tightening. The calculation model is shown in Fig. 2.

Based on the constant unstrained length, mass conservation, and deformation compatibility conditions, an algorithm for analysing the influence of strand sag on cable shape during erection is established according to Eqs. (1) and (2). The specific steps are as follows.

- (1) Given the number of strands (n), strand sag (f_i), elastic modulus (E), steel wire diameter (d), height difference (Δh) and horizontal distance (L) between points A and B, the initial unit self-weight (q_{0i}), maximum tension (T_{0i}) and unstrained length (s_{0i}) of each strand are calculated, where i ranges from 1 to n .
- (2) Assume that the uniform sag of each strand after cable tightening is $f_0 = (f_{\max} + f_{\min})/2$, where f_{\max} and f_{\min} represent the maximum and minimum sags of all strands, respectively.
- (3) Solve for the unit self-weight (q_i) of each strand after cable tightening based on the unstrained length (s_{0i}) and initial sag (f_{0i}).
- (4) Calculate $\Delta q = \sum_{i=1}^n q_i - \sum_{i=1}^n q_{0i}$.
- (5) According to the principle of mass conservation, the convergence condition ($|\Delta q| < \varepsilon$) is determined, where the calculation accuracy (ε) is assumed to be $10e-5$. If $|\Delta q| < \varepsilon$ the sag of the main cable after cable tightening is f_0 , otherwise the sag after cable tightening is recalculated according to the sag increment (Δf), i.e., $f_0 = f_0 + \Delta f$.
- (6) Repeat steps 3 to 5 until $|\Delta q| < \varepsilon$ is satisfied.

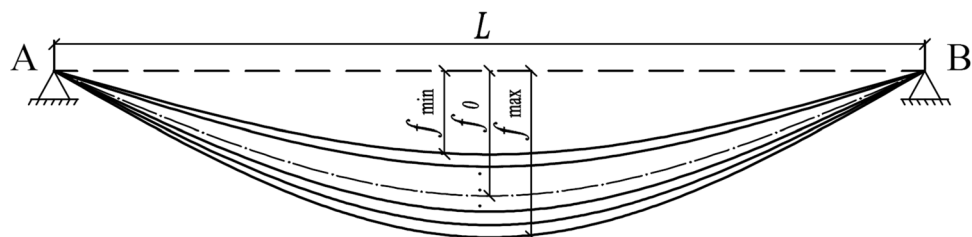


Figure 2. Model schematic.

- (7) Output the sag of the main cable (f_0) and the maximum tension of each strand (T_i) after cable tightening.

According to the above steps, an analysis program for determining the impact of the inter-strand distance on the cable shape is compiled using MATLAB, and the analysis flow is shown in Fig. 3.

Program verification

To verify the correctness of the program, three strands are used for the calculation of cable tightening. The span (L) and theoretical sag of the strand (f_0) are 922.261 m and 83.258 m respectively. The strand is composed of 91 steel wires. The elastic modulus (E) and diameter (d) of the steel wire are 201.635 GPa and 5.019 mm, respectively. The unit self-weight (q_0) of the strand is 0.1413 kN/m. The sags of the three strands before cable tightening are $f_1 = 82.958$ m, $f_2 = 83.258$ m, and $f_3 = 83.558$ m. The main cable sag (f_0), unit self-weight (q), and maximum tension (T) of the strand after cable tightening are calculated and shown in Table 2.

Table 2 shows that the uniform strand sag (f_0) after cable tightening is 83.2583 m, which is in excellent agreement with the theoretical value. The sum of the unit self-weight and total tension of the three strands after

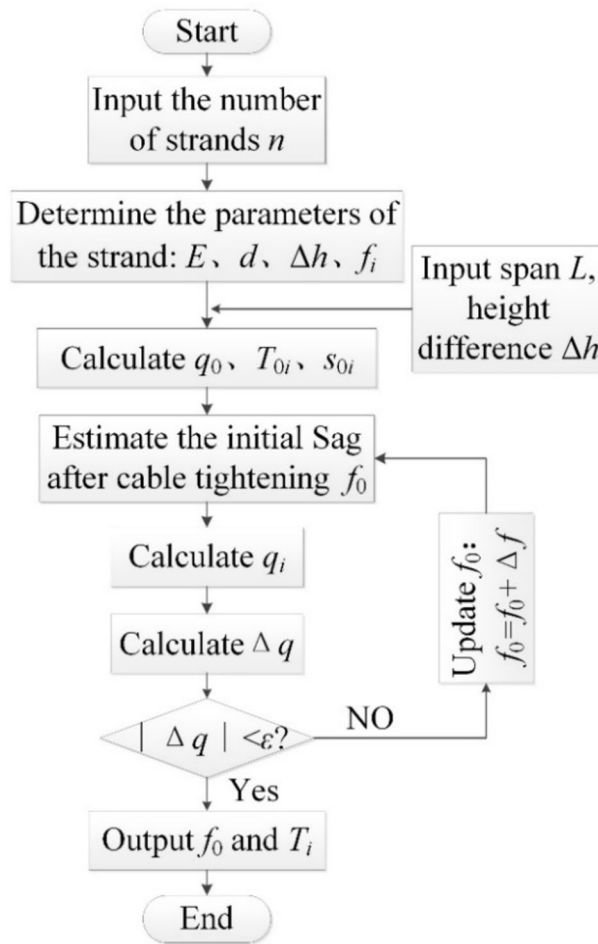


Figure 3. Analysis flow of the inter-strand distance on the cable shape.

Strand number	Before cable tightening			After cable tightening		
	f_i (m)	q_0 (kN/m)	T (kN)	f_0 (m)	q (kN/m)	T (kN)
1	82.958	0.1413	194.66	83.2583	0.1828	250.99
2	83.258	0.1413	194.05		0.1414	194.10
3	83.558	0.1413	193.45		0.0998	137.04
Total		0.4239	582.16		0.4239	582.14

Table 2. The calculated results.

cable tightening is the same as that before cable tightening, thus confirming the consistency with the theoretical analysis results. This finding verifies the accuracy of the program.

Research on methods for controlling strand sag Engineering case

This paper examines the impact of different sag control methods on the main cable shape and strand tension after cable tightening, using a double-tower single-span ground-anchored suspension bridge in Yunnan Province, China, as a case study. The bridge has a main cable span arrangement of 255 m + 920 m + 255 m, with a rise-span ratio of 1/10 (Fig. 4). It consists of two main cables, each comprising 154 prefabricated parallel steel wire strands, as shown in Fig. 5. Each strand is a regular hexagon, composed of 91 steel wires with a diameter of 5.019 mm and an elastic modulus of 201.635 GPa. The bulk density of the steel wire is 78.5 kN/m³. Due to the pre-deviation of the saddle, the main span measures 922.261 m, and the side span measures 253.084 m at the time of strand erection. The theoretical unstrained lengths of the main span and the side span are 941.525 m and 277 m, respectively.

Methods for controlling strand sag

Based on previous project investigations^{6,11,17,19,20}, four methods of strand sag control during the main cable erection process have been summarized (Fig. 6). Method I involves controlling the spacing of the strands according to the principle of “half approaching, half separation”, with each strand’s sag set to the theoretical value. The existence of errors will make the erection quality of this method unsatisfactory. Method II raises all strands as a whole by a value of d . Although this method reduces the possibility of the main cable shape being lower than desired compared to Method I, it is difficult to accurately obtain the value of d . Method III raises all the strands except the reference strand by a value of d . This method can better ensure that the reference strand is in the theoretical position, so the quality of strand erection can be checked at any time. Method IV involves raising each strand layer by layer, with each upper layer raised by a value of d compared to the adjacent lower layer. Method IV protects the reference strand better than the other three methods. However, due to the large spacing of the strands, it is difficult to tighten the cable and the strand tension varies greatly.

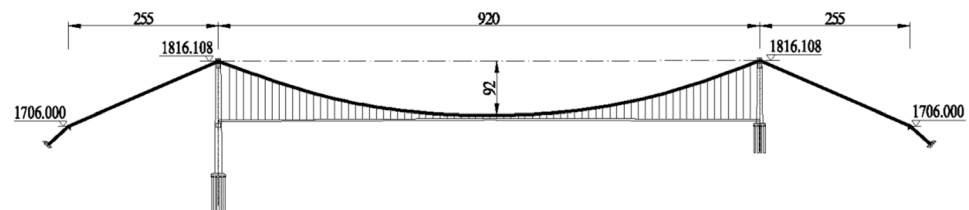


Figure 4. Overall layout of the bridge. (Units: m).

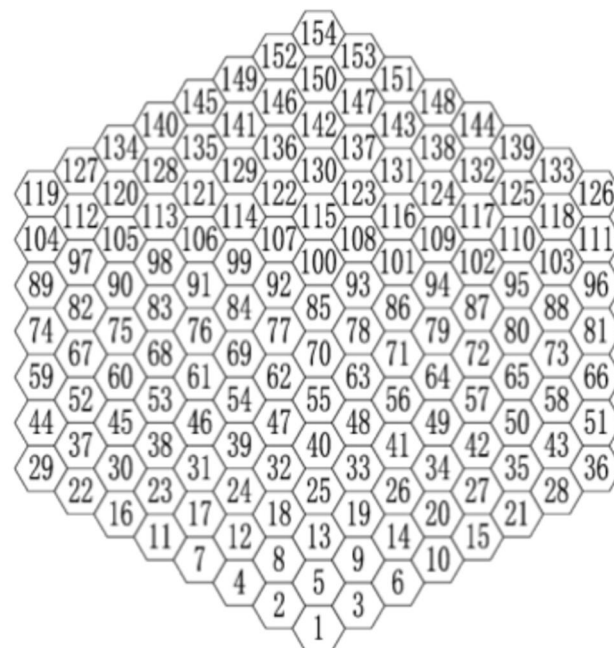


Figure 5. Section of the main cable and strand number.

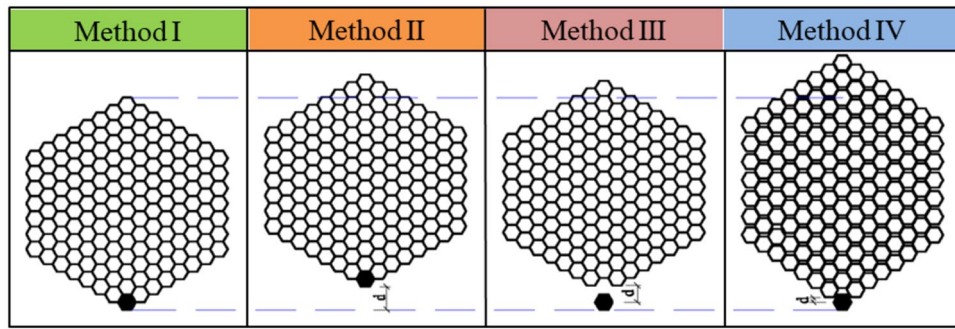


Figure 6. Various methods for controlling strand sag.

Deterministic analysis

In this section, the four control methods are individually analysed using the aforementioned bridge as a calculation example. Only the value of the inter-strand distance d will change, while the other parameters will remain at the theoretical values. In Methods I to III, the value of d does not exceed 10 cm, while in Method IV, it does not exceed 1 cm. Method III was used in the engineering case, and the value of d was 2 cm. The strand sag (f_0) (Fig. 7) and strand maximum tension (T_i) (Figs. 8, 9 and 10) in the main span and side span after cable tightening are calculated.

The theoretical values of the strand sag (f_0) obtained from Method I are 83.258 m for the main span and 11.594 m for the side span. Figure 7 shows that all control methods have a linear relationship between f_0 and d . Methods II and III have the same linear rate of change, while Method IV has the largest. Additionally, the influence of d on the strand sag in the main span and side span follows the same pattern.

The theoretical value of the strand maximum tension (T_i) obtained from Method I is 194.05 kN for the main span and 125.54 kN for the side span. All strands in Method II have the same tension after cable tightening. Figure 8 indicates a linear relationship between T_i and d , with the side span exhibiting a greater linear change rate than the main span.

Method III only lifts the general strand as a whole, so the tension of all strands except the reference strand is consistent after cable tightening. Figure 9 demonstrates that the tension difference (ΔT) between the reference

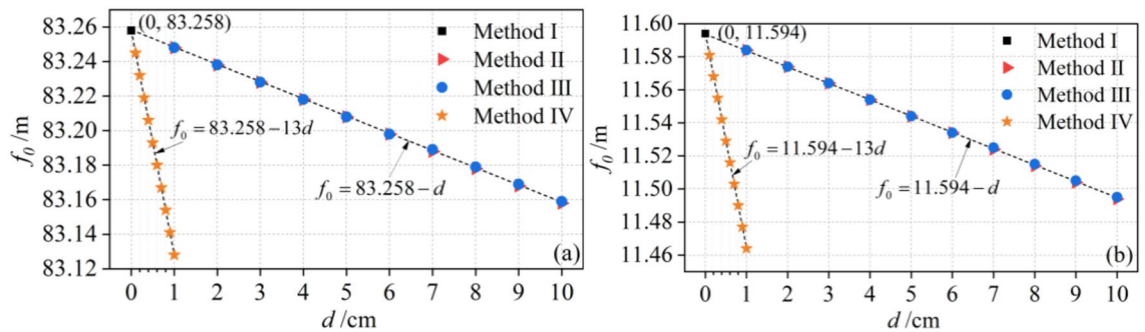


Figure 7. The strand sag (f_0) after cable tightening for all methods: (a) main span, and (b) side span.

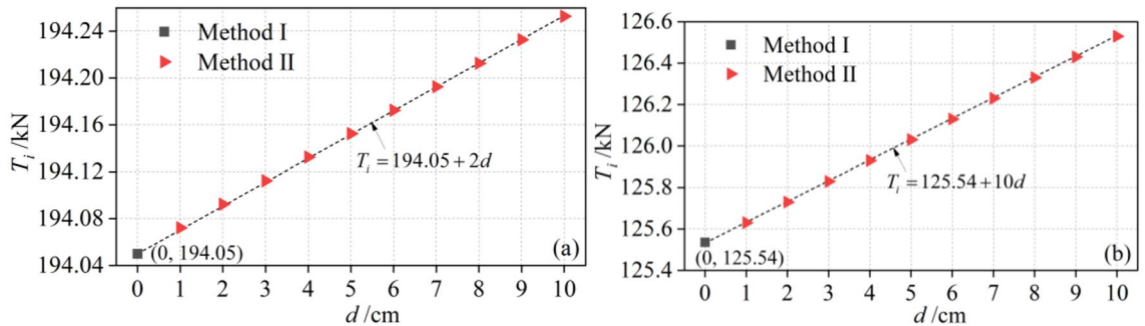


Figure 8. The maximum strand tension (T_i) after cable tightening for Methods I and II: (a) main span, and (b) side span.

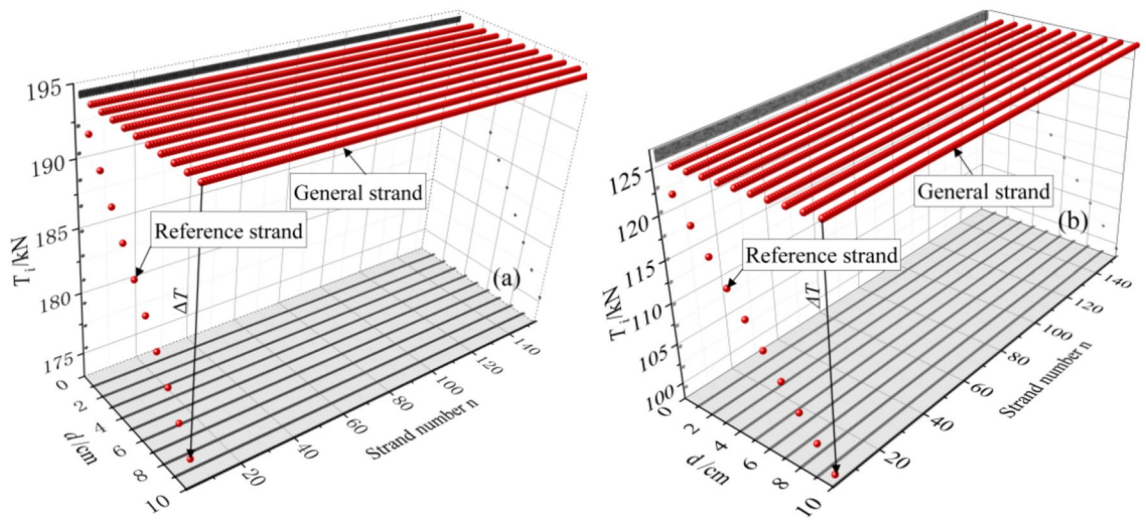


Figure 9. The maximum strand tension (T_i) after cable tightening for Method III: (a) main span, and (b) side span.

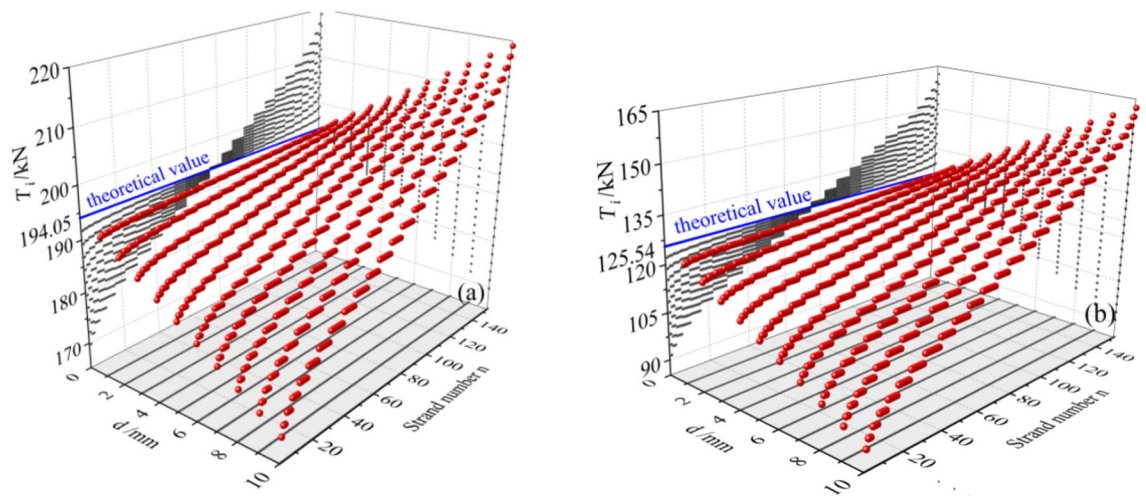


Figure 10. The strand maximum tension (T_i) after cable tightening via Method IV: (a) main span, and (b) side span.

strand and the general strand is linearly related to d , i.e., for every 1 cm increase in d , ΔT increases by 1.90 kN and 2.74 kN for the main span and side span, respectively.

Each layer of strands in Method IV has a different sag and therefore a different tension. As shown in Fig. 10, larger values of d lead to greater deviations in strand tension from the theoretical value. The non-uniformity (δ) is used to indicate the degree of tension inconsistency among the strands after cable tightening, $\delta = (\Delta T/T) \times 100\%$, where ΔT represents the difference between the maximum and minimum values of the strand tension, and T denotes the average value of tension. Further calculation reveals an approximately linear relationship between δ and d , where the main span and side span are represented as $\delta = 25.4d$ and $\delta = 55.8d$, respectively. The existence of an erection error leads to different unstrained lengths of strands, which leads to differences in tension between strands after cable tightening. Therefore, the overall tensile stiffness of the main cable will change, and the unstrained length of the main cable will no longer be consistent with the theoretical value, which will change the overall mechanical performance of the main cable.

Uncertainty analysis

Determination of random variables

Factors such as variations in wire material properties, measurement levels, and temperature differences make it difficult to accurately control the strand spacing. Therefore, it is necessary to analyse the influence of these random factors on the four control methods and understand the structural behavior from a probabilistic perspective. The elastic modulus (E) and diameter (d) of the steel wire, the span (L), the height difference of the support point (Δh), the absolute sag error (Δf_1), the absolute temperature error (t_1), the relative sag error (Δf) and the relative temperature difference (Δt) of the general strand are regarded as random variables, and each random

variable is considered independent of the others. To obtain an accurate statistical characterization of these random variables, extensive statistical work was conducted in the field. Specifically, the distribution characteristics of the elastic modulus and diameter of steel wires were obtained via random sampling. Two full-time surveyors alternately and continuously measured the fixed measuring points to obtain the distribution characteristics of the elevation, mileage and temperature parameters on windless nights. The statistical results are shown in Table 3.

Theoretical model of cable tightening considering random factors

According to the process of strand erection, a quantitative analysis model was developed to analyse the influence of different sag control methods on cable shape and tension, taking into account random factors. The model considers the errors of each strand separately and uses Latin hypercube sampling to sample all random variables to ensure reliable calculations. The specific steps involved in the calculation are as follows:

- (1) Erection of the reference strand: Random sampling is performed for the variables L , Δh , Δf_1 and t_1 from Table 3. The elastic modulus (E_1), diameter (d) and unstrained length (s_1) of the reference strand are kept at the theoretical values. Subsequently, the target control value for the main span sag (f_1) is calculated. Considering the measurement errors, the actual sag value (f_i) of the reference strand, denoted as $f_1 = f_1 + \Delta f_1$, is obtained. The erection of the reference strand is completed.
- (2) Erection of general strands: The sag control method and the elevation value (ΔD) of each strand are determined, and the measurement error (Δf_i) is randomly sampled to obtain the true sag value (f_i), where $f_i = f_1 + \Delta D + \Delta f_i$. Random sampling is performed for Δt_i , E_i , and d_i , and the theoretical values of L and Δh are used to calculate the actual unstrained length (s_i) of each strand.
- (3) Cable tightening: This part is consistent with section “Calculation principle and program implementation” and will not be repeated. The Monte Carlo method is utilized to repeat steps (1) to (3) N times, and the sag (f_0) and maximum tension (T_i) of the strand after cable tightening are recorded. The analysis program is compiled using MATLAB based on the above steps, and the calculation process is illustrated in Fig. 11.

Calculated results

In analysing the abovementioned bridge as a case study, the four control methods were examined individually. Comparing the calculation results for sample sizes $N=200$ and $N=300$, it was observed that the two statistical results exhibited minimal differences. Thus, $N=200$ was chosen for further statistical analysis. Table 4 provides a comparison of a portion of the calculated results for the strand sag and tension non-uniformity after cable tightening of the main span.

The value of the parameter d aligns with the deterministic analysis. The mean and standard deviation of the sag and tension non-uniformity in the strand after cable tightening were calculated. The calculated results for the main span are illustrated in Figs. 12 and 13.

Considering the influence of random factors, it was found that the strand sag after cable tightening follows a normal distribution. Figure 12 demonstrates that the mean sag values for the four methods are consistent with the deterministic analysis results described in section “Deterministic analysis”, and the relationships with parameter d also remain consistent. At a confidence level of 95%, the confidence interval of Method I ($d=0$) varies between 83.245 m and 83.271 m. Similarly, at the same confidence level, the confidence intervals of Methods II and III are identical to that of Method I, indicating that parameter d affects only the mean of the sag and not its dispersion. Method IV has a relatively larger value of σ_{f_0} than Method I, II and III but it is independent of the magnitude of d .

Considering the influence of random factors, the non-uniformity of the strand maximum tension after cable tightening follows a normal distribution. Figure 13 indicates that the non-uniformity obtained by Method I ($d=0$) is between [4.87%, 7.49%] at a confidence level of 95%. This non-uniformity is primarily influenced by the statistical characteristics of random factors (Table 3), and the calculated results closely align with those of Method II. Method III exhibits higher non-uniformity compared to Method I, mainly due to the tension difference between the reference strand and the general strand, with an exponential relationship between μ_δ and d . When $d=2$ mm, the value of σ_δ is similar to that of Method I primarily because of the small value of d , with σ_δ being primarily affected by random factors. However, when $d=4$ mm to 10 mm, the larger value of d causes its

Construction steps	Error factors	Main span		Side span		Distribution
		Mean	Standard deviation	Mean	Standard deviation	
Reference strand erection	L (m)	922.261	0.002	253.084	0.002	Normal
	Δh (m)	0	0.003	110.108	0.003	Normal
	Δf_1 (m)	0	0.002	0	0.002	Normal
	t_1 (°C)	0	0.192	0	0.192	Normal
General strands erection	Δf (m)	0	0.0017	0	0.0017	Normal
	Δt (°C)	0	0.495	0	0.495	Normal
Cable tightening	E (GPa)	201.635	0.298	201.635	0.298	Normal
	d (mm)	5.019	0.0014	5.019	0.0014	Normal

Table 3. Statistical characteristics of random variables.

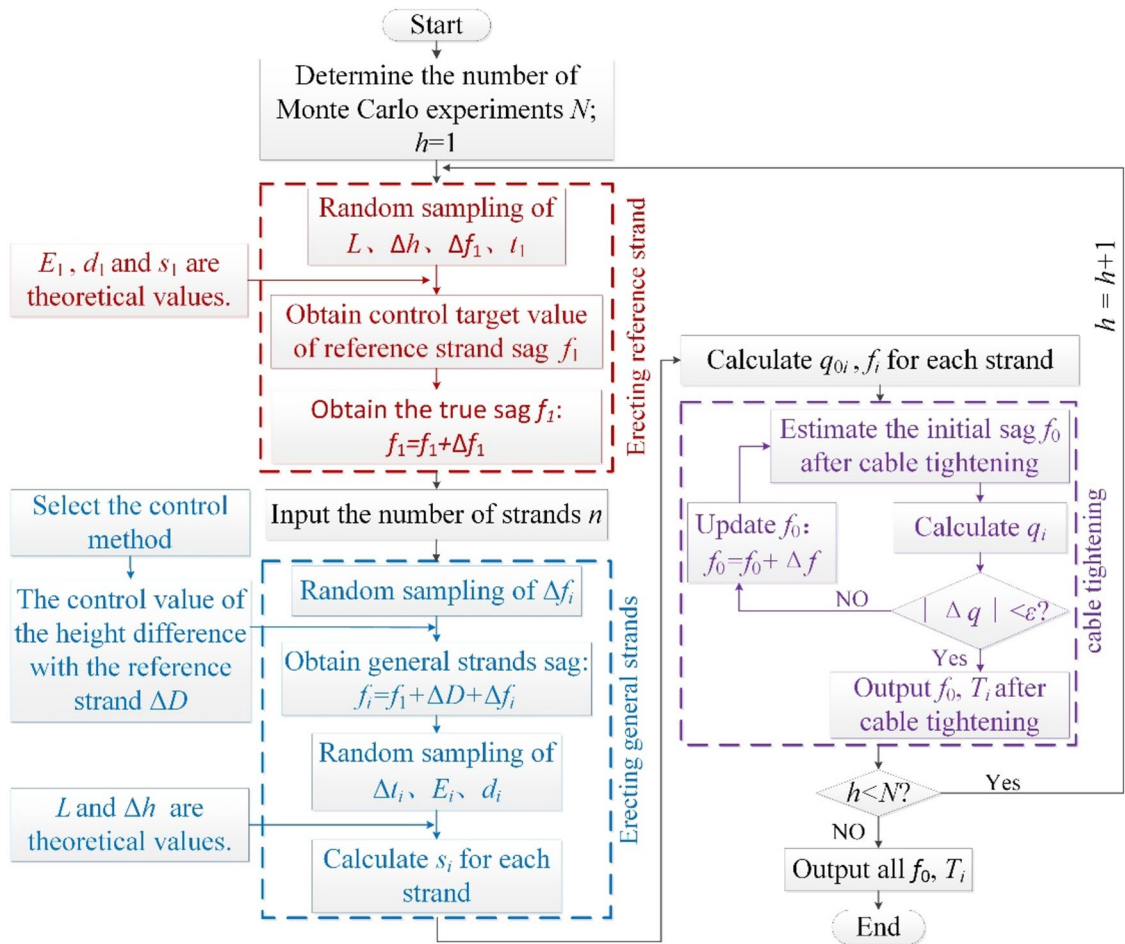


Figure 11. The flow for analysing the effect of the sag control method on the main cable shape considering random factors.

	j_0 (m)		δ ($\times 100\%$)		j_0 (m)		δ ($\times 100\%$)	
	μ_{f_0}	σ_{f_0}	μ_δ	σ_δ	μ_{f_0}	σ_{f_0}	μ_δ	σ_δ
	Method I ($d=0$ cm)				Method II ($d=10$ cm)			
$N=200$	83.258	0.0065	6.18	0.67	83.158	0.0067	6.25	0.71
$N=300$	83.258	0.0066	6.20	0.69	83.158	0.0066	6.22	0.70
	Method III ($d=10$ cm)				Method IV ($d=1$ cm)			
$N=200$	83.158	0.0066	12.85	0.50	83.128	0.0085	26.23	1.25
$N=300$	83.158	0.0066	12.88	0.48	83.128	0.0083	26.25	1.28

Table 4. Comparison of calculation results for different sample sizes.

influence on tension uniformity to surpass the impact of random factors, resulting in σ_δ being slightly smaller than that of Method I. The μ_δ of Method IV also increases exponentially with increasing d . The μ_δ and σ_δ are the largest among the four methods. Because the strands of this method are raised layer by layer, the interaction between the strands increases the degree of dispersion. The variance reflects the dispersion degree of the cable shape and the uneven tension among the strands after cable tightening. The larger the variance is, the more unstable the construction quality of the main cable is, and it may even exceed the specified limit.

Discussion and summary

Based on the calculation results, in the deterministic analysis, Method I represents the ideal state where the sag and tension of each strand are theoretical values. Method II, on the other hand, affects only the cable sag and overall tension of the strand, which change linearly with parameter d . Because there are no gaps between the strands in Method II, the strand tension is uniform. Method III involves lifting the general strand as a whole,

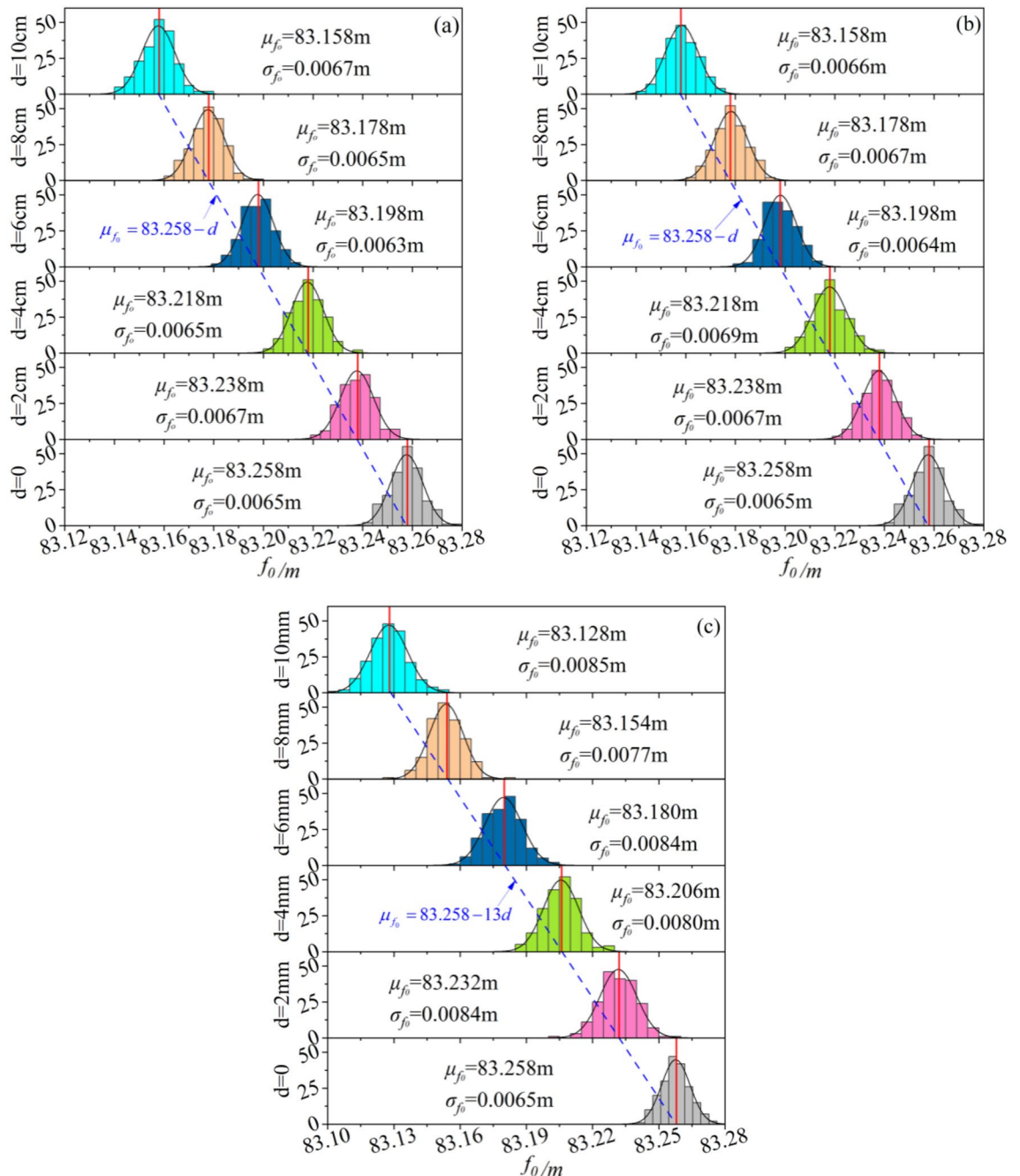


Figure 12. Strand sag (f_0) after cable tightening for Methods II to IV: (a) Method II, (b) Method III, and (c) Method IV.

and since the proportion of a single reference strand is very small, its results are similar to those of Method II. However, there is a difference in the tension of the reference strand after cable tightening, which is lower than that of the general strand, and the tension difference is proportional to the amount of lifting. In Method IV, the sag of each layer of strands differs, leading to inconsistent tension among the layers, with the unevenness of tension proportional to parameter d .

It is important to note that the presence of random errors can make it challenging to erect strands according to the accurate elevation. In the uncertainty analysis, the sag and tension non-uniformity of the four methods are normally distributed. Although the mean value of the sag is consistent with the deterministic analysis, random errors can cause the actual cable sag to deviate from the theoretical value. Methods I to III have similar dispersions due to sag control based on the reference strand. However, Method IV, which relies on adjacent layers as a reference for strand erection, tends to accumulate errors between layers, resulting in relatively greater sag dispersion.

Random errors can also increase the unevenness of tension. Similar to Method I, Method II, is influenced only by random factors, and the unevenness of tension is unrelated to the lifting value. In Method III, due to the

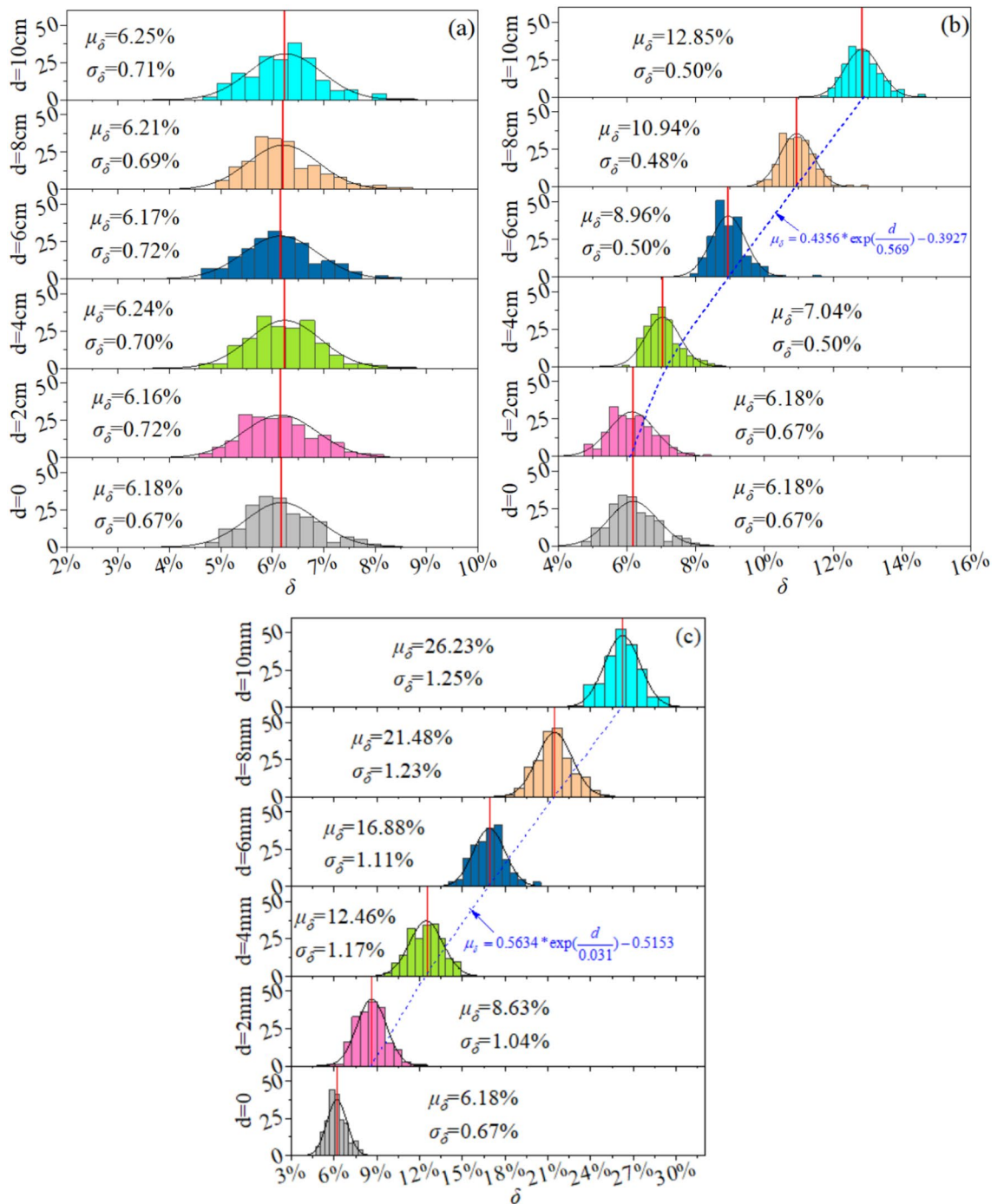


Figure 13. Non-uniformity (δ) of the strand maximum tension after cable tightening for Methods II to IV: (a) Method II, (b) Method III, and (c) Method IV.

increased distance between the reference strand and the general strand, the tension gap between them widens, and this effect gradually increases with distance. Due to the influence of random factors, lifting amount, and cumulative effects of errors between layers, Method IV exhibits the highest level of non-uniformity in strand tension and the greatest degree of dispersion.

The above analysis results are applicable to both the main span and the side span. The strand tension in the side span, however, is significantly more affected than that in the main span. To provide a clear overview, the characteristics of the four methods are summarized in Table 5.

Based on these findings, the following suggestions are proposed for the four control methods:

- (1) During the main cable construction process, it is crucial to consider not only the main cable shape but also the uniformity of strand tension. The appropriate method should be chosen based on the control standards.

Method	Characteristics	Method	Characteristics
I	Sag deviation: not large Uniformity of tension: relatively uniform Reference strand compression: easy	II	Sag deviation: larger Uniformity of tension: relatively uniform Reference strand compression: easy
III	Sag deviation: larger Uniformity of tension: the tension of the general strand is relatively uniform Reference strand compression: not easy	IV	Sag deviation: largest Uniformity of tension: uneven Reference strand compression: not easy

Table 5. The characteristics of the four methods.

- (2) The inter-strand distance should not be increased indiscriminately to prevent compression of the reference strand.
- (3) Regardless of the method used, reducing the impact of random factors is essential for improving cable shape accuracy.
- (4) It is recommended that the reference strand be used as a guide for erecting cables to avoid mutual interference between layers.
- (5) Method III has good performance in terms of both the main cable shape and uniformity of tension, but the value of d should be reasonably determined according to the actual situation of the project.

However, only a single project has been analysed in this paper, and the effects of different spans and different numbers of strands should also be considered to better guide the construction. Whether the potential contact between individual strands changes the load on each strand is not discussed in the paper, and will be considered in future research.

Conclusions

In this paper, we summarize four sag control methods based on existing engineering cases and compile an influence analysis program to examine the cable shape and internal force of the strand for each control method. Taking a suspension bridge as a case study, the following conclusions are drawn:

- (1) Deterministic analysis.
In Method I, the sag and tension of each strand are at their theoretical values, representing the ideal state. Method II exhibits a linear relationship between the main cable sag and the lifting value, with uniform tension in the strands. The cable sag calculation results of Method III are consistent with those of Method II, but as the elevation increases, the difference in the tension between the reference strand and the general strand also increases. Method IV shows the largest deviation from the theoretical values, both in strand sag and tension, with the deviation directly proportional to the interlayer spacing.
- (2) Uncertainty analysis.
The cable sag and tension non-uniformity of the four control methods are normally distributed. Although the mean value of the main cable sag is consistent with the results of the deterministic analysis, there is a certain level of dispersion in the calculated cable sag due to random factors. The comparison of dispersion is as follows: Method I = Method II = Method III < Method IV. The tension non-uniformity of Method II is similar to that of Method I and is independent of the lifting value. The non-uniformity of tension in Methods III and IV shows an exponential relationship with the lifting value. When the degree of influence of the elevation is lower than that of random factors, the standard deviation of the tension uniformity in Method III is close to the calculated result of Method I. Conversely, when the elevation has a greater influence, it is lower than that in Method I. Method IV has the largest mean and standard deviation of the tension non-uniformity among the four methods.
- (3) The reference strand of method I is easy to press, which makes the cable shape more difficult to control. The pre lifting amount of method II is difficult to determine, and the final cable shape is difficult to predict. Method III has better performance in terms of the main cable shape and tension uniformity, and the value of d is the key. Method IV can better protect the reference strand, but the final main cable shape and tension uniformity are sensitive to the prelifting amount.

Data availability

The datasets used and analysed during the current study available from the corresponding author on reasonable request.

Received: 27 September 2023; Accepted: 19 July 2024

Published online: 27 July 2024

References

1. Sun, Y. M., He, X. D. & Li, W. D. Influential parameter study on the main-cable state of self-anchored suspension bridge. *KEM* **619**, 99–108 (2014).

2. Zhang, W., Li, T., Shi, L., Liu, Z. & Qian, K. An iterative calculation method for hanger tensions and the cable shape of a suspension bridge based on the catenary theory and finite element method. *Adv. Struct. Eng.* **22**, 1566–1578 (2019).
3. Kim, H. S., Kim, Y. J., Chin, W. J. & Yoon, H. Development of highly efficient construction technologies for super long span bridge. *Engineering* **05**, 629–636 (2013).
4. Huang, P. & Li, C. Review of the main cable shape control of the suspension bridge. *Appl. Sci.* **13**, 3106 (2023).
5. Konishi, I. Latest developments on prefabricated parallel wire strand in Japan. *Ann. Ny. Acad. Sci.* **352**, 55–70 (1980).
6. Matsuzaki, M., Uchikawa, C. & Mitamura, T. Advanced fabrication and erection techniques for long suspension bridge cables. *J. Constr. Eng. Manag.* **116**, 112–129 (1990).
7. Zhou, X. & Zhang, X. Thoughts on the development of bridge technology in China. *Engineering* **5**, 1120–1130 (2019).
8. Zhang, W., Shi, L., Li, L. & Liu, Z. Methods to correct unstrained hanger lengths and cable clamps' installation positions in suspension bridges. *Eng. Struct.* **171**, 202–213 (2018).
9. Chen, Y., Wei, W. & Dai, J. The key quality control technology of main cable erection in long-span suspension bridge construction. *IOP Conf. Ser. Earth Environ. Sci.* **61**, 012124 (2017).
10. Wang, Z. Construction monitoring techniques for superstructure of Yingwuzhou Changjiang River Bridge in Wuhan. *Bridge Constr.* **48**, 100–105 (2018).
11. Xu, T., Zhang, Y. S. & Zeng, X. Influence of construction error on suspender length of suspension bridges. *J. Chongqing Jiaotong Univ. (Nat. Sci.)* **32**, 915–917 (2013).
12. Li, J., Li, A. & Feng, M. Q. Sensitivity and reliability analysis of a self-anchored suspension bridge. *J. Bridge Eng.* **18**, 703–711 (2013).
13. Li, H., Xian, Z. Q., Shen, L. C., Wen, W. & Dong, T. Method of adjusting cable strand sagging for suspension bridge of Runyang Bridge. *Bridge Constr.* **2004**, 36–39 (2004).
14. Bi, X. D., Feng, Y. X. & Yang, M. Technical improvement and construction of main cable strand erection of Ma Anshan Bridge. *J. Highw. Transp. Res. Dev. (Appl. Technol.)* **10**, 215–218 (2014).
15. Li, H. The main cable erection technology for preventing the main cable of suspension bridge from bulging and twisting. *Chin. Overseas Architect.* **2015**, 177–178 (2015).
16. Liao, C., Zhang, N. L. & Yi, J. W. The main suspension cable erection technology of Aizhai Bridge. *Constr. Technol.* **42**, 5–8 (2013).
17. Feng, C. B. Control techniques for superstructure construction of Wu Fengshan Yangtze River Bridge. *Bridge Constr.* **50**, 99–104 (2020).
18. Ministry of Transport of China. Technical specifications for construction monitoring and control of highway bridges, JTG/T3650-01-2022, Beijing (2022).
19. Zhao, Y. *Research on Main Cable Control and Poisson Effect Involved in Suspension Bridge* (Chang'an University, 2016).
20. Zhang, W., Liu, Z. & Xu, S. Jindong bridge: Suspension bridge with steel truss girder and prefabricated RC deck slabs in China. *Struct. Eng. Int.* **29**, 315–318 (2019).
21. Xiao, R., Chen, M. & Sun, B. Determination of the reasonable state of suspension bridges with spatial cables. *J. Bridge Eng.* **22**, 04017060 (2017).
22. Wang, X. *et al.* Form-finding method for the target configuration under dead load of a new type of spatial self-anchored hybrid cable-stayed suspension bridges. *Eng. Struct.* **227**, 111407 (2021).
23. Li, T. & Liu, Z. An improved continuum model for determining the behavior of suspension bridges during construction. *Automat. Constr.* **127**, 103715 (2021).
24. Zhu, W., Ge, Y., Fang, G. & Cao, J. A novel shape finding method for the main cable of suspension bridge using nonlinear finite element approach. *Appl. Sci.* **11**, 4644 (2021).
25. Li, T., Liu, Z. & Zhang, W. Analysis of suspension bridges in construction and completed status considering the pylon saddles. *Eur. J. Environ. Civ. En.* **26**, 4280–4295 (2022).
26. Deng, X. & Deng, H. Improved algorithm to determine the composite circular curve splay saddle position. *Struct. Eng. Int.* **33**(1), 141–146. <https://doi.org/10.1080/10168664.2021.2004975> (2022).
27. Shen, R. L., Ye, Z. L., Shen, W. & Tang, M. L. Research on construction control parameters of wire strands of main cable. *J. Archit. Civil Eng.* **27**, 13–18 (2010).

Acknowledgements

This research was supported by the National Key R&D Program of China (2019YFB1600702).

Author contributions

P.H. conceived the idea of the article and analyzed the data, and also provided financial support for the work. C.L. wrote the main manuscript text. H.X. supervised the manuscript. All authors reviewed the manuscript.

Competing interests

The authors declare no competing interests.

Additional information

Correspondence and requests for materials should be addressed to C.L.

Reprints and permissions information is available at www.nature.com/reprints.

Publisher's note Springer Nature remains neutral with regard to jurisdictional claims in published maps and institutional affiliations.



Open Access This article is licensed under a Creative Commons Attribution-NonCommercial-NoDerivatives 4.0 International License, which permits any non-commercial use, sharing, distribution and reproduction in any medium or format, as long as you give appropriate credit to the original author(s) and the source, provide a link to the Creative Commons licence, and indicate if you modified the licensed material. You do not have permission under this licence to share adapted material derived from this article or parts of it. The images or other third party material in this article are included in the article's Creative Commons licence, unless indicated otherwise in a credit line to the material. If material is not included in the article's Creative Commons licence and your intended use is not permitted by statutory regulation or exceeds the permitted use, you will need to obtain permission directly from the copyright holder. To view a copy of this licence, visit <http://creativecommons.org/licenses/by-nc-nd/4.0/>.

© The Author(s) 2024